

1-1-2012

A comparison of spatially explicit and classic regression modelling of live coral cover using hyperspectral remote-sensing data in the Al Wajh lagoon, Red Sea

S Hamylton

University of Wollongong, shamylto@uow.edu.au

Follow this and additional works at: <https://ro.uow.edu.au/scipapers>



Part of the [Life Sciences Commons](#), [Physical Sciences and Mathematics Commons](#), and the [Social and Behavioral Sciences Commons](#)

Recommended Citation

Hamylton, S: A comparison of spatially explicit and classic regression modelling of live coral cover using hyperspectral remote-sensing data in the Al Wajh lagoon, Red Sea 2012, 2161-2175.
<https://ro.uow.edu.au/scipapers/4781>

Research Online is the open access institutional repository for the University of Wollongong. For further information contact the UOW Library: research-pubs@uow.edu.au

A comparison of spatially explicit and classic regression modelling of live coral cover using hyperspectral remote-sensing data in the Al Wajh lagoon, Red Sea

Abstract

Live coral is a key component of the Al Wajh marine reserve in the Red Sea. The management of this reserve is dependent on a sound understanding of the existing spatial distribution of live coral cover and the environmental factors influencing live coral at the landscape scale. This study uses remote-sensing techniques to develop ordinary least squares and spatially lagged autoregressive explanatory models of the distribution of live coral cover inside the Al Wajh lagoon, Saudi Arabia. Live coral was modelled as a response to environmental controls such as water depth, the concentration of suspended sediment in the water column and exposure to incident waves. Airborne hyperspectral data were used to derive information on live coral cover as a response (dependent) variable at the landscape scale using linear spectral unmixing. Environmental controls (explanatory variables) were derived from a physics-based inversion of the remote-sensing dataset and validated against field-collected data. For spatial regression, cases referred to geographical locations that were explicitly drawn on in the modelling process to make use of the spatially dependent nature of coral cover controls. The transition from the ordinary least squares model to the spatially lagged model was accompanied by a marked growth in explanatory power ($R^2 = 0.26$ to 0.76). The theoretical implication that follows is that neighbourhood context interactions play an important role in determining live coral cover. This provides a persuasive case for building geographical considerations into studies of coral distribution.

Keywords

spatially, explicit, classic, modelling, live, coral, cover, hyperspectral, regression, remote, comparison, sensing, data, al, wajh, lagoon, red, sea

Disciplines

Life Sciences | Physical Sciences and Mathematics | Social and Behavioral Sciences

Publication Details

Hamylton, S. (2012). A comparison of spatially explicit and classic regression modelling of live coral cover using hyperspectral remote-sensing data in the Al Wajh lagoon, Red Sea. *International Journal of Geographical Information Science*, 26 (11), 2161-2175.

1 A comparison of spatially explicit and classic regression modelling 2 of live coral cover using hyperspectral remote sensing data in the 3 Al Wajh lagoon, Red Sea

4 Abstract

5 Live coral is a key component of the Al Wajh marine reserve in the Red Sea, and the management of this reserve
6 is dependent on a sound understanding of the existing spatial distribution of live coral cover and the
7 environmental factors influencing live coral at the landscape scale. The present study uses remote sensing
8 techniques to develop ordinary least squares and spatially lagged autoregressive explanatory models of the
9 distribution of live coral cover inside the Al Wajh lagoon, Saudi Arabia. Live coral was modelled as a response
10 to environmental controls such as water depth, the concentration of suspended sediment in the water column and
11 exposure to incident waves. Airborne hyperspectral data were used to derive information on live coral cover as a
12 response (dependent) variable at the landscape scale using linear spectral unmixing. Environmental controls
13 (explanatory variables) were derived from a physics-based inversion of the remote sensing dataset and validated
14 against field-collected data. For spatial regression, cases referred to geographical locations that were explicitly
15 drawn on in the modelling process to make use of the spatially dependent nature of coral cover controls. The
16 transition from the ordinary least squares model to the spatially lagged model was accompanied by a marked
17 growth in explanatory power ($R^2=0.26$ to $R^2=0.76$). The theoretical implication that follows is that
18 neighbourhood context interactions play an important role in determining live coral cover. This provides a
19 persuasive case for building geographical considerations into studies of coral distribution.

20 *Keywords: Spatial regression, Saudi Arabia, spatial autoregression, spatial autocorrelation,*
21 *live coral cover*

22 1 Introduction

23 Coral reefs underpin tropical coastal ecosystems through the provision of ecological services (e.g.,
24 mangrove and seagrass growth promotion, structural habitat complexity for fish) and goods (e.g.,
25 primary production to support fish and invertebrate populations, calcification) (Côté and Reynolds,
26 2006). To sustain these goods and services, marine protected areas have been proven a highly effective
27 conservation measure for coral reefs (Roberts et al., 2003). At the heart of marine protected area
28 planning is the need to understand both the existing spatial distribution of live coral and the

29 environmental factors influencing their distribution at the landscape scale (10 – 100 km²) (Sobel &
30 Dahlgren, 2004; Almany et al., 2009). One of the key challenges to the development of this
31 understanding is the paucity of biophysical datasets available in these frequently large but remote
32 environments. Recent increases in the accuracy, precision and affordability of geospatial technologies
33 (GIS, GPS and remote sensing) provide new opportunities for mapping and modelling live coral cover.
34 Such technologies yield geographically-referenced datasets that allow mapping and modelling
35 exercises to be conducted in a spatially explicit manner. This allows reef managers to quantify spatial
36 patterning in benthic communities, determine optimal sampling strategies for monitoring ecological
37 health and avoid the incorporation of redundancy into datasets (which in turn violates statistical
38 assumptions about the geographical independence of benthic communities across reefs) (Haining,
39 2003).

40

41 Mapping the distribution of live coral cover has largely been made possible through the development
42 of optical satellite and airborne as well as acoustic remote sensing technology and the associated
43 refinement of image processing routines for application to marine environments. Airborne
44 hyperspectral remote sensing campaigns acquire imagery of the requisite spatial and spectral detail to
45 accurately resolve live coral while accounting for the influence of the overlying atmospheric and water
46 column layers on light transfer (Klonowski et al, 2007). The rich content of hyperspectral datasets
47 allows their manipulation to retrieve information on water quality, bathymetry and benthic cover using
48 physics-based inversion techniques (Brando et al., 2009; Hedley et al 2009), spectral unmixing
49 (Goodman and Ustin, 2007), optimization and semi-analytical techniques (Lee et al. 1999; Wettle et
50 al. 2006). Such mapping exercises yield spatially continuous, landscape scale datasets on the
51 distribution of live coral that can be used as a foundation for modelling exercises that further our
52 understanding of the relationship between live coral cover and local environmental influences.

53

54 Spatial modelling can be defined as an assemblage of empirical techniques in which a clear
55 association is maintained and exploited between quantitative data and the spatial coordinates that
56 locate them (Chorley 1972). Defined in this way, the application of spatial modelling has largely
57 developed through the establishment of spatially explicit rule sets for defining segments of object-

58 based image analysis techniques (Benfield et al. 2007) and the use of spatial metrics to quantify spatial
59 patterning on reefs (Le Drew et al. 2000; Phinn et al. 2003; Purkis et al. 2007). In terms of inferential
60 modelling that seeks to explain or predict observable patterns in live coral cover, classic (spatially
61 implicit) statistical approaches have commonly been employed at the landscape scale, such as ordinary
62 least squares regression (Harborne et al, 2006) and generalised additive models (Garza Perez, 2004).
63 Such approaches do not account for the inherent spatial structure of ecosystems (Fortin and Dale,
64 2005) that is manifest on a coral reef as a result of the autocorrelated distribution of the environmental
65 characteristics that determine coral survival.

66

67 The objective of this study is to use hyperspectral remote sensing techniques to implement and
68 compare two different multivariate regression models that seek to explain the spatial distribution of
69 live coral cover inside a lagoon at the landscape scale. A wide variety of controls could potentially
70 influence the proportion of live coral cover inside the Al Wajh lagoon. These include, but are not
71 limited to, water depth, wave power, suspended sediment concentration, the frequency and intensity of
72 high energy storm events, the availability of antecedent platform and suitable substrate for larval
73 settlement (for a comprehensive summary of environmental controls of coral distribution, see Done,
74 2011). These controls operate across a range of scales and while some are subject to local fluctuations
75 that produce interrelationships, synergies and feedbacks, others (e.g. salinity) can be considered
76 uniform across the extent of the study area and treated as constant terms. Of these variables, water
77 depth, wave power and suspended sediment concentration were selected for the models because they
78 have been suggested as determinants of coral community structure inside the Al Wajh lagoon
79 (Sheppard et al. 1992; De Vantier 2000). They also exhibit variation at the scale of the study area and
80 information on these variables can be derived at the landscape scale across the study area using GIS
81 and remote sensing techniques.

82

83 A key aim of this study is to establish which type of regression modelling is most appropriate for
84 explaining the distribution of live coral inside the Al Wajh lagoon. One model uses ordinary least
85 squares regression while a second introduces a spatially lagged autoregressive term to build a spatial

86 component into the model. The null hypothesis for these models is that none of the variables have any
87 influence on the distribution of live coral cover inside the Al Wajh lagoon.

88 **2 Methodology**

89 **2.1 Study Area**

90 The Al Wajh Bank is situated along the north-eastern part of the Red Sea coastline of the Kingdom of
91 Saudi Arabia (Figure 1), it is the most extensive of a series of reef platforms that comprise a reserve
92 network designated by the National Commission for Wildlife Conservation and Development in 2000.
93 The modelling exercise aimed to develop an understanding of the environmental controls on live coral
94 distribution to inform reserve management. It was applied to a sub-area of interest at the northern end
95 of the lagoon which traversed environmental gradients of water depth, suspended sediment
96 concentration and wave exposure (see inset box on Figure 1).

97

98 The barrier reef system is comprised of a continuous line of reefs stretching for approximately 100 km
99 and separated by several narrow (< 200 m width) channels. The outer edge of the bank lies
100 approximately 26 km offshore and runs parallel to the shoreline for approximately 50 km before
101 curving landward to enclose the reef system around a central lagoon (Fig. 1). The depth of the lagoon
102 floor ranges from 30-60 m, becoming progressively shallower towards the coastline that comprises an
103 alluvial sandy plain. The present living reefs, both along the barrier and inside the lagoon, have
104 developed during the past 6000 years as Holocene sea levels have risen on top of topographic highs
105 formed by earlier reef structures (Sheppard et al. 1992; De Vantier 2000). The shelf inside the barrier
106 supports a range of islands and associated reef formations including platform or patch reefs, lagoon
107 pinnacles, reticulate reef systems, submerged reef ridges and cay reefs.

108

109 [Figure 1 here]

110 **2.2 Methodology**

111 The methodological components of this study can be subdivided into two sections: *i.* the derivation
112 and validation of variables using remote sensing techniques and *ii.* The construction and comparison
113 of two different types of regression model (classic and spatially explicit) for live coral cover.

114 [Figure 2 here .]

115

116 **2.3 The derivation and validation of variables using remote sensing techniques**

117

118 *2.3.1 Acquisition of airborne hyperspectral imagery*

119

120 Hyperspectral data inside the Al Wajh barrier were acquired on 9th May 2008 using an AISA Eagle

121 imaging sensor mounted to a Cessna seaplane. The AISA Eagle instrument measured 128 contiguous

122 spectral bands from 400 to 994 nm at a spectral and spatial resolution of 5 nm and 1 m respectively.

123 The image covered approximately 20 km² (1.5 km wide by 13 km in length) and was located along the

124 northern coast of the inner Wajh Barrier.

125

126 **2.4 Derivation of information on explanatory variables: Water depth, suspended**

127 **sediment concentration and wave exposure**

128 *2.4.1 Water depth and suspended sediment concentration*

129

130 An atmospheric correction was carried out on the raw hyperspectral imagery using the fast-line-of-

131 sight atmospheric analysis of spectral hypercubes (FLAASH) moduleTM within the software

132 environment for visualising images (ENVI) 4.5. Standard atmospheric water column amounts were

133 calculated for a tropical atmosphere with a maritime aerosol model to represent the boundary layer

134 above oceans, accounting for sea spray (Cooley et al. 2002).

135

136 A semi-analytical optimization model was used to simultaneously derive bathymetry, water optical

137 properties and subsurface remote sensing reflectance from the atmospherically corrected hyperspectral

138 image. The semi-analytical model algorithm was based on quasi-single-scattering theory (Gordon,

139 1994), and was implemented through a series of simulations that populated parameters to estimate

140 subsurface remote sensing reflectance from surface remote sensing reflectance (Lee et al. 1998 and

141 1999). To perform the optimisation it was necessary to impose a series of constraints on input

142 parameters, the derivation of which are outlined by Goodman et al. (2008), who describe the

143 application of this approach to a coral reef environment (Table 1). For the purpose of this analysis, the

144 model was applied to coral spectra to yield information on bottom albedo, the particle-backscattering

145 coefficient (from which a measure of suspended sediment could be derived) and water depth.

146
147
148
149
150
151

Table 1. Constraints employed for optimisation of the semi-analytical inversion model, as defined in Goodman (2008).

152 *2.42 Field measurement of water depth and suspended sediment*

153 A dataset of 188 bathymetric readings across the study area was collected using a Norcross X single
154 beam bathymetric sounder in conjunction with the water sampling for validating the output
155 bathymetry from the semi-analytical model. The suspended sediment concentration (SSC) was
156 measured *in-situ* by extracting 50 water samples of 200 mL volume from transects ran perpendicular
157 to the coastline across the coastal shelf. Sample collection was timed to coincide with acquisition of
158 the airborne remotely sensed imagery and extractions were taken from just below the wave base at a
159 depth of 1 m using a length of piping with a pre-rinsed sample bottle attached to the end of it. The
160 location of each sample was recorded using a dGPS (accuracy < 1 m).

161

162 Suspended sediment was measured from the field samples in a laboratory using filtration methods. For
163 estimation of SSC across the study area, the dataset of fifty water samples was divided randomly so
164 that 25 of the samples could be used to establish a simple power relationship between the particle
165 backscattering coefficient (derived from the semi-analytical optimization modelling) and suspended
166 sediment. This relationship was then used to predict suspended sediment concentration across the
167 study area using ArcGIS Model Builder. The remaining 25 samples were used to test the accuracy of
168 this relationship once it had been extrapolated over the study area. This validation proceeded by
169 plotting the locations of the field samples taken and comparing suspended sediment measured in the
170 laboratory with that modelled from the remote sensing image.

171

172 *2.4.3 Wave Exposure model*

173 To estimate wave exposure, the fetch-based method of Ekeboom et al. (2003) was employed using
174 linear wave theory to estimate incident power on the basis of fetch and wind power statistics, with
175 bathymetric information incorporated to account for the influence of refraction and shoaling (for

176 further details of method see Hamylton, 2011b). A 30 m grid was placed over the study area and the
177 radiating lines extension tool in ArcView (Jenness 2006) was used to generate 8 lines of length 30 km,
178 spaced 45 degrees apart, originating from each grid point. All fetch-limited lines (i.e., those
179 intersecting an overlaid coastline shapefile) were trimmed at the point of intersection with the
180 coastline. Polyline lengths were then calculated and input as fetch distances from each direction into
181 the linear wave transform model.

182

183 Data on the speed and frequency of direction from which winds blew in the study area were extracted
184 from the Indian Ocean volume of the *Marine Climatic Atlas of the World* (United States Navy 1995)
185 for input into the linear wave transform model. This atlas reported wind speed and frequency data
186 from a meteorological station at 10m above sea level approximately 50 km north of the study site
187 located on Bahrein Island, Saudi Arabia (26°16'N, 50° 37'E). Data were averaged across a time period
188 that spanned from January 1991-October 1995.

189

190 Fetch lengths and wind data were input into the significant wave height and wave period equations
191 which were used to calculate wave energy from linear wave theory (Ekebom et al. 2003; Hamylton,
192 2011b). As the study area was inside an enclosed lagoon, fetch-limited equations were employed for
193 each cardinal and subcardinal direction and summed to provide an overall measure of exposure at each
194 grid point, which was then interpolated to a continuous surface of 1 m resolution.

195 **2.5 Derivation of information on the Dependent variable: live coral cover**

196

197 *2.5.1 Field sampling of image spectra and coral community surveys*

198 Field spectra of four benthic coverages (live coral, dead coral, macroalgae and sand) were collected
199 for input to the spectral unmixing algorithm using a TRIOS™ Ramses ARC sensor. These coverages
200 were representative of the community components falling inside the study area on habitat maps
201 previously prepared by the Japanese International Cooperation Agency through interpretation of aerial
202 photography. The spectrometer measured light in the wavelength range 300 - 920 nm, with an optical
203 resolution of ~5 nm (Datentechnik GmbH, 2004). Underwater measurements were taken across an
204 integration time of 63 ms with 50 replications collected for each benthic coverage within each of five

205 sample sites. Average endmember spectra for each target were smoothed for the elimination of high
 206 frequency noise (Savitzky-Golay, 1964) and interpolated to yield reflectance at 1 nm intervals with a
 207 cubic spline (Karpouzli *et al.*, 2004).

208
 209 Additional coral community records were collected in the form of six detailed 20 x 2 m phototransects
 210 established across a range of inshore - offshore and sheltered – exposed locations. This methodology
 211 yielded 20 photographs per transect line, i.e., 120 photographs overall, each of which were visually
 212 assessed for percentage of live coral cover using Coral Point Count with single random point
 213 specification (Kohler and Gill 2006).

214 215 *2.5.2 Spectral unmixing of the hyperspectral imagery*

216
 217 A brief summary of the unmixing routine applied to the hyperspectral imagery is provided here as a
 218 detailed description has been published elsewhere (Hamylton, 2011a). Pre-processing steps included
 219 atmospheric and water column correction (see section 2.4.1), geometric correction and data subsetting
 220 via multiple discriminant function analysis. Multiple discriminant function analysis was applied to the
 221 collected field spectra to define an optimal subset of wavelengths for resolving benthic coverages and
 222 spectral unmixing was performed on this subset to decompose the reflectance of the materials with
 223 different spectral properties inside the ground field of view of a single pixel (1 x 1 m resolution)
 224 (Kruse *et al.* 1993). On the basis of the image reflectance for each pixel and the field collected spectra
 225 of the individual benthic coverages, the proportions of the individual elements falling inside each pixel
 226 were derived by solving a set of simultaneous linear equations. The linear mixture model assumed
 227 that, for a given wavelength, the total number of photons reflected from a single pixel and detected by
 228 the sensor was a linear function of the reflectance of the individual components and the fractional area
 229 of the pixels they cover:

$$230 \quad r_x = \sum_{j=1}^n a_{xi} f_j + e_x \quad \text{Equation 1}$$

231
 232 where r_x = reflectance of a given pixel in the xth of z spectral bands

233 n = the number of mixture components

234 f_j = the jth fractional component in the makeup of r_x

235 a_{xy} = the reflectance of mixture component j in spectral band x

236 e_x = the difference between the pixel reflectance and that computed from the model.

237 Unmixing accuracy was assessed using a combination of the root mean square error model and
238 comparison against the field data collected using the phototranssects. The overall root mean square
239 error was calculated as the difference between the reflectance measured by the sensor and that
240 computed from the unmixing algorithm, this was averaged for each waveband independently.

241 Comparisons against field data proceeded via a linear regression between the actual proportion (as
242 estimated from the phototranssect mosaic) and the estimated proportion (from spectral unmixing).

243 The output image depicting the derived spatial patterns of abundance for live coral across the study
244 area was treated as a representation of the response variable for input into the regression models.

245

246 **2.6 The construction and comparison of classic and spatially explicit regression models** 247 **for live coral cover.**

248 The spatial structure of the coral coverage dataset was explored by converting the unmixed coral cover
249 layer to a point file and computing the local Geary's C statistic as a measure of spatial autocorrelation
250 between all pairs of points. A semivariogram was generated to determine the optimum sampling grid
251 size at which there was no spatial dependence between the data points and therefore no internal
252 redundancy. An exponential model was found to best fit the dataset with spatial dependency reaching
253 a sill at 30 m distance between points. To represent coral cover (the dependent variable of the model),
254 a 30m grid of coverage values was therefore extracted by overlaying a grid of points spaced 30 m
255 apart and taking an average value of a 3 by 3 cell window from the unmixed coral cover layer (1m
256 resolution) as input to the regression modelling exercise. Corresponding values were extracted for
257 each of the explanatory variables (water depth, suspended sediment concentration and wave exposure)
258 at each grid point location, each of which represented a data case.

259

260 Two regression procedures were carried out using the derived data cases in the software GeoDa
261 (Anselin, 2003). These were ordinary least squares (classic) regression and spatially lagged
262 autoregression. After confirmation that the raw data complied with the assumptions of regression, the

263 two types of regression analysis were carried out in sequence to measure the proportion of variation in
 264 coral cover accounted for by each model. In the second regression model, spatial structure was
 265 included via the introduction of a spatially lagged autoregressive term as an explanatory variable. This
 266 approach drew explicitly on the location of each individual case through the construction of a spatial
 267 weights matrix ($w_{(i,j)}$) that expressed for each data case whether or not other cases belonged to its
 268 neighbourhood, such that $w_{ij}=1$ when i and j were neighbours and $w_{ij}=0$ otherwise (Anselin and Bera
 269 1998). The values of the dependent variable at neighbouring locations were therefore introduced into
 270 the standard regression equation:

$$271 \mu_{(i)} = \beta_0 + \beta_1 X_{1(i)} + \beta_2 X_{2(i)} + \beta_3 X_{3(i)} + \rho \sum_{j \in N(i)} w(i,j) Y(j) + e_{(i)} \quad i = 1, \dots, n \quad \text{Equation 2}$$

273 where n = the number of points or areas

274 $X_1 - X_3$ are the explanatory variables,

275 $e(i)$ = independent, normally distributed error term

276 β_0 to β_k = coefficients estimated using the model.

277 ρ = a parameter associated with the interaction effect.

278

279 To estimate the spatial autoregressive terms in the spatial lag model, all cases and the spatial weights
 280 matrix were input into a maximum likelihood procedure that generated consistent estimates of ρ and β .
 281 A distinguishing feature of the likelihood for linear regression parameters with a spatial autoregressive
 282 component is a Jacobian term of the form $|I - \rho W|$, an evaluation of which was carried out based on
 283 the characteristic polynomial of the spatial weights matrix, W , to maximise the likelihood function of
 284 this term. This approach was originally suggested by (Ord 1975) and was developed into an efficient
 285 computer algorithm in the software GeoDa (Smirnov and Anselin 2001). After each regression
 286 analysis, diagnostics were recorded (including the Moran's I statistic, t-test, and measures of fit) and
 287 the spatial distribution of model residuals was mapped. A model building approach was taken whereby
 288 a range of independent variables were employed in the initial runs, with analysis of the t-statistic
 289 providing justification for retaining some variables and excluding others future runs. For example,
 290 both phytoplankton backscatter and dissolved organic matter were taken out of the model after initial
 291 runs as they did not make a statistically significant contribution to the performance of the model.

292

293 **3 Results**294 **3.1 Derivation of information on explanatory variables: Water depth, suspended**
295 **sediment concentration and wave exposure**

296 The bathymetric map revealed that water depths inside the study area ranged between 0.2m above reef
297 patches and 30m inside the channel towards the northern end of the study area. These closely
298 approximated the 188 values measured *in-situ* with a bathymetric sounder (R^2 0.95). In the broader
299 context of the Al Wajh reef system, the deep channel towards the north of the study area leads to a
300 large opening in the northern barrier wall, one of only two sites of water exchange between the lagoon
301 and outside ocean waters. The shallower areas of the study site coincided with the platform in the
302 north, the ridge network and the tops of the patches in the south.

303

304 Suspended sediment values measured from the water samples extracted inside the lagoon ranged
305 between 5 and 73 mg L⁻¹. The distribution indicated that suspension of sediments coincided with
306 shallower areas. The association between the particle backscatter coefficient estimated from the
307 imagery and sediment content of the water was strong (R^2 0.91 based on the 25 samples).

308

309 The wave power model distribution was elevated over the ridge towards the north of the study area
310 immediately below an opening in the Wajh Bank. The majority of the study area was fetch-limited,
311 being surrounded by the Wajh Bank to the west and the mainland to the east. However, one small area
312 in the north of the study area is non fetch-limited in a northerly direction. Power levels ranged between
313 2 and 699 Jm⁻³ throughout the study area.

314 **3.2 Derivation of information on the Dependent variable: live coral cover**

315

316 The two hundred and fifty reflectance spectra collected showed considerable variability between the
317 spectra of the different benthic coverages, each of which had their own unique reflectance curve. The

318 airborne dataset was reduced from 128 bands to 27 discriminant functions composed of reflectance
319 and first order derivative spectra, as identified by the multiple discriminant function analysis. For the
320 field sites where the coral community was sampled via phototransects, the cover of live coral ranged
321 from 30-74% (Figure 3).

322

323 [Figure 3 here]

324

325 On the spectrally unmixed output coverage, white areas that indicated high coral cover coincided with
326 coral that was visible on the three band pseudocolour image (Fig. 4a) and the overall root mean
327 square error was low (<0.01). Estimates of live coral cover correlated strongly with field assessments
328 (R^2 0.89) and were elevated in three general areas. Firstly, to the north of the study area around the
329 periphery of the shallow bank (although not across the shallow top of this, an area which is exposed at
330 low tide). Secondly, several prominent ridges of high live coral cover stood out among the network
331 across the centre of the study site. Thirdly, areas of interspersed high coral cover were present in
332 conjunction with the patches in the south of the study site.

333

334 [Figure 4 here]

335 **3.3 The construction and comparison of classic and spatially explicit regression models** 336 **for live coral cover.**

337

338 All of the input variables were significant and the ordinary least squares and spatially lagged
339 regression models explained 26 % and 76 % respectively of the variation in live coral cover inside the
340 study area. For both models, water depth was negatively correlated and suspended sediment and wave
341 exposure were positively correlated with live coral cover. Suspended sediment had the highest t-
342 statistic in both cases, which was notably higher in the ordinary least squares model, with depth and
343 wave power contributing less explanatory power. Nonetheless, the t-test values suggested that each
344 variable was significant ($p<0.001$) and it follows that their contribution to the overall live coral
345 coverage model was valuable, providing a statistical justification for rejecting the null hypothesis. The

346 test for multicollinearity revealed minimal association between these distinct explanatory variables of
347 the dataset. The residuals from the ordinary least squares regression model displayed strong positive
348 spatial structure, which was corroborated by the Moran statistic (Table 2). For the spatially lagged
349 model, weak negative autocorrelation was apparent.

350 **Table 2** Summary of results and diagnostics for the two types of regression.

351 **4 Discussion**

352 The moderate T-statistic for water depth was not in agreement with other coral reef studies which
353 identify this as a key determinant of coral cover (Done, 2011; Kleypas et al. 1999). This is perhaps
354 because of its status as an indirect variable, or environmental proxy, in marine environments. Potential
355 controlling variables for which depth could act as a surrogate include temperature, light availability
356 and degree of atmospheric exposure. These may mask or altogether counteract each other by exerting
357 opposing influences on live coral cover. Processes may also interact in a non-linear manner along a
358 depth gradient to cancel each other out in terms of their effects on live coral coverage. For example,
359 coral cover may be highest at a depth where the mechanical disturbance caused by wave interaction is
360 moderate at an intermediate disturbance level (Aronson and Precht 1995). Such a pattern could not be
361 captured in a regression model.

362
363 The concentration of suspended sediment explained the highest proportion of variation, with higher
364 concentrations associated with greater proportions of live coral cover. Although the presence of
365 sediments is generally an impediment to coral survival because of abrasion and smothering, they are
366 less likely to stress corals when strong currents are present (Rogers, 1990). Fine material (<0.15 mm
367 diameter) rarely settles in waters of velocity 25 cm s^{-1} , rather it stays uniformly entrained throughout
368 the fluid (Komar 1976). Wajh lagoon sediments (which were consistently found to be <0.15 mm in
369 diameter) likely stay suspended in shallower water of elevated velocity at a concentration too low to
370 impede photosynthesis. Furthermore, the association of food particulates that favour coral growth such
371 as zooplankton and dissolved organic matter with suspended sediment might benefit heterotrophic
372 corals that feed directly from the water column (Johannes et al. 1970).

373

374 Wave power explained the least amount of variation in live coral cover, likely because of a trade-off
375 between the constructive and destructive influence of water movement on coral. While circulation
376 replenishes food and oxygen provision and removes metabolic waste products (Birkeland 1996), it
377 also presents a mechanical stress whereby shallow benthic communities must withstand the force of
378 breaking waves to persist (Massel 1996).

379

380 In the presence of spatial dependence, the initial ordinary least squares model inflated the goodness of
381 fit measure and underestimated the standard error, increasing the likelihood of a Type I error (Cliff
382 and Ord 1981). Failure to include spatial autocorrelation in the specification meant that some of the
383 effect due to interaction would have been allocated to the existing covariates, particularly those with a
384 similar spatial structure to the response variable. Respecification to incorporate a neighbourhood
385 context effect operating through a spatially lagged expression of the response variable itself allowed
386 this to be addressed. This neighbourhood context effect might be underpinned by either ecological
387 factors, such as coral community reproduction, geomorphological ones, such as the presence of
388 antecedent platform. In the Red Sea, endogenous influences could include a relatively short planktonic
389 life cycle phase of around 35-40 days (Rinkevich and Loya 1979) and structural support provided by
390 the existing structure of primary reef framework (Goreau 1959). Over longer timescales this latter
391 influence may be perpetuated by regional variability of eustatic sea level, which spreads alluvial
392 material from adjacent mountain ranges smothering reef and encouraging contemporary corals to grow
393 on the elevated platforms of their Pleistocene counterparts (Shaked and Genin, 2011; Hayward 1982).
394 Scaling up to the interaction of multiple corals, ecological processes such as the spread of disease and
395 competition for light are known to have a characteristic spatial structure (Fortin and Dale, 2005). The
396 action of any of these influences would associate the presence of nearby live corals on the reef with
397 existing live coral coverages, as demonstrated by the autoregressive model.

398

399 The study exemplifies the degree to which hyperspectral data can be manipulated to support spatially-
400 explicit modelling in coral reef environments. Extended coverage of the electromagnetic spectrum
401 underpinned much of the modelling process with different dimensions of this dataset to providing
402 critical information on water depth, suspended sediment concentration and coral cover. Unmixing

403 algorithms that treated the data as spectrally continuous yielded outputs at the *ratio* level of
404 measurement (i.e. a continuous map of the percentage of live coral cover across the study area). This
405 added versatility to the modelling process by extending the range of statistical techniques available for
406 realising explanatory power through the model. The value of introducing a spatial component was
407 demonstrated for a number of reasons, including *i.* identification of an appropriate sampling scale for
408 model development, *ii.* use of spatially lagged information (i.e., from a neighbouring site) on the
409 response variable itself to increase explanatory model power, and *iii.* detection of spatial dependence
410 (autocorrelation) in the model. Nonetheless, each of the image processing steps from which the
411 dependent and explanatory variables were derived (pre-processing, inversion, unmixing etc.)
412 introduced an element of uncertainty into the models applied. While validation and accuracy
413 assessment exercises permitted comparison of model outputs with values observed *in-situ*, an
414 awareness of the cumulative influence of uncertainty along the analysis chain, for example, error in
415 inversion and unmixing closure, is important. The study presented here could profitably be improved
416 by a further error propagation or sensitivity analysis (Schott 2007).

417

418 **Conclusion**

419 A key aim of this study was to establish which type of regression modelling is most appropriate for
420 explaining the distribution of live coral inside the Al Wajh lagoon. To do so, it is useful to distinguish
421 between determinants that reflect endogenous interaction between the sites and those that respond to
422 some other exogenous variable. Assessing the relative contribution of effects caused by a reaction to
423 external forces and effects that are a reaction to neighbouring individuals determines the
424 appropriateness of the model specified. When external forces are the major influence, a classic
425 ordinary least squares regression model is appropriate, whereas interactive effects suggest a need for a
426 model with a spatially dependent covariance structure (Hamylton, 2011c; Cliff and Ord 1981).
427 Transition to a model that incorporated spatial dependence was accompanied by a marked growth in
428 explanatory power. The theoretical implication that follows is that neighbourhood interactions play a
429 more important role than previously thought. This invites greater consideration of explanatory

430 variables that reflect interaction between sites, providing a persuasive case for explicitly building
 431 geographical considerations into studies of coral distribution.

432

433 **Acknowledgements**

434 This work would not have been possible without the generous support of the Khaled bin Sultan Living
 435 Oceans Foundation. Dr Tom Spencer at the University of Cambridge is thanked for guidance on the
 436 manuscript and Dr Rainer Reuter, University of Oldenburg and the National Coral Reef Institute,
 437 Nova Southeastern University are thanked for assistance with fieldwork.

438 **6.0 References**

- 439 Almany G.R., Connolly S.R., Heath D.D., Hogan J.D., Jones G.P., McCook L.J., Mills M., Pressey
 440 R.L., Williamson D.H.. Connectivity, biodiversity conservation and the design of marine reserve
 441 networks for coral reefs. *Coral Reefs*, 2009; 28, 339–351.
- 442 Anselin L., Bera A. (1998). Spatial dependence in linear regression models with an introduction to
 443 spatial econometrics. In: Ullah A, Giles DE (Eds), *Handbook of applied economic statistics*. New
 444 York: Marcel Dekker Press.
- 445 Anselin L. (2003) GeoDa™ 0.9 User's Guide. Illinois: Centre for Spatially Integrated Science.
- 446 Aronson R.B., Precht W.F. (1995). Landscape patterns of reef coral diversity: A test of the
 447 intermediate disturbance hypothesis, *Journal of Experimental Biology and Ecology*, 192, 1-14.
- 448 Benfield S.L., Guzman H.M., Mair J.M., Young J.A.T. (2007). Mapping the distribution of coral reefs
 449 and associated sublittoral habitats in Pacific Panama: a comparison of optical satellite sensors and
 450 classification methodologies. *International Journal of Remote Sensing*, 28, 5047-5070.
- 451 Birkeland C. (1996). Life and death of coral reefs. New York: Chapman and Hall.
- 452 Brando, VE, Anstee, JM, Wettle, M, Dekker, AG, Phinn, SR & Roelfsema, C (2009) A physics based
 453 retrieval of quality assessment of bathymetry from suboptimal hyperspectral data, *Remote Sensing of*
 454 *Environment*, 113, 755-700.
- 455 Chorley R.J.E. (1972). Spatial analysis in geomorphology. London: Methuen Press.
- 456 Cliff A.D., Ord J.K. (1981). Spatial processes: models & applications. London: Pion.
- 457 Cooley T., Anderson G.P., Felde G.W., Hoke M.L., Ratkowski A.J., Chetwynd J.H., Gardner J.A.,
 458 Adler-Golden S.M., Matthew M.W., Berk A., Bernstein L.S., Acharya P.K., Miller D., Lewis P
 459 (2002). FLAASH, A MODTRAN-4 based atmospheric correction algorithm, its application and
 460 validation. Proceedings of the Geoscience and Remote Sensing Symposium, 2002, Toronto, Canada,
 461 3, 1414 – 1418.
- 462 Côté, IM, Reynolds, JD (2006) Coral Reef Conservation, Cambridge University Press, Cambridge
- 463 Datentechnik GmbH (2004). Ramses Hyperspectral Radiometer Manual Release 1.0,
- 464 De Vantier L. (2000). Final report on the study on coastal marine habitats and biological inventories in
 465 the northern part of the Red Sea coast in the Kingdom of Saudi Arabia. Report to the National
 466 Commission for Wildlife Conservation and Development, Riyadh, Saudi Arabia, Japan International
 467 Cooperation Agency.
- 468 Done, T. (2011) Corals: Environmental Controls on Growth. In: Hopley D (ed) Encyclopedia of Modern Coral
 469 Reefs. Springer, Dordrecht, The Netherlands, p 281.

- 470 Doxoran, D., Froidefond, J., Lavendar, S. & Castaing, P. (2002). Spectral signature of highly turbid
 471 waters; application with SPOT data to quantify suspended particulate matter concentrations. *Remote*
 472 *Sensing of Environment*, 81, 149-161.
- 473 Ekeboom J., Laihonon P., Suominen T. (2003) A GIS-based step-wise procedure for assessing physical
 474 exposure in fragmented archipelagos. *Estuarine and Coastal Shelf Science*, 57, 887-898
- 475 Fortin M-J., Dale M.R.T. (2005). Spatial analysis: a guide for ecologists. Cambridge: Cambridge
 476 University Press.
- 477 Garza-Perez, J.R., Lehmann, A., Arias-Gonzalez, J.E. (2004). Spatial prediction of coral reef habitats:
 478 integrating ecology with spatial modelling and remote sensing, *Marine Ecology Progress Series*, 269,
 479 141-152.
- 480 Gordon, H.R. (1994). Modeling and simulating radiative transfer in the ocean. Chapter 1 in *Ocean*
 481 *Optics*, R.W. Spinrad, K.L. Carder and M.J. Perry (Eds), Oxford: Oxford University Press.
- 482 Goodman, J & Ustin, S.L. (2007) Classification of benthic composition in a coral reef environment
 483 using spectral unmixing, *Journal of Applied Remote Sensing*, 1, 011-501.
- 484 Goodman, J., Lee Z.P. & Ustin, S. (2008). Influence of atmospheric and sea-surface corrections on
 485 retrieval of bottom depth and reflectance using a semi-analytical model: a case study in Kaneohe Bay,
 486 Hawaii. *Applied Optics*, 47, 1-11
- 487 Goreau T.F. (1959). The ecology of Jamaican coral reefs. I. Species composition and zonation.
 488 *Ecology* 40, 67-90
- 489 Hamylton, S. (2011a). Estimating the coverage of coral reef benthic communities in the Al Wajh, Red
 490 Sea from airborne hyperspectral remote sensing data: Multiple discriminant function analysis and
 491 linear spectral unmixing. *International Journal of Remote Sensing*, 32: 9673 - 9690.
- 492 Hamylton, S. (2011b). The use of remote sensing and linear wave theory to model local wave energy
 493 around Alphonse Atoll, Seychelles. *Estuarine, Coastal and Shelf Science*, 95, 349-358
- 494 Hamylton, S (2011c) The Al Wajh Bank reef system, Saudi Arabia, Red Sea, pp. 28 – 37. In: Harris, P
 495 & Baker, E (Eds.) (2009) Atlas of Seafloor Geomorphology as Habitat, Elsevier, Chatswood,
 496 Australia. 600pp.
- 497 Haining, R. (2003) Spatial Data Analysis: Theory and practice. Cambridge: Cambridge University
 498 Press.
- 499 Harborne A.R., Mumby P.J., Zychaluk K., Hedley J.D., Blackwell P.G. (2006). Modeling the beta
 500 diversity of coral reefs. *Ecology* 87, 2871-2881.
- 501 Hayward A.B. (1982). Coral reefs in a classic sedimentary environment: Fossil (Miocene, SW Turkey)
 502 and Modern (Recent, Red Sea) analogues. *Coral Reefs*, 1, 109-114.
- 503 Hedley, J, Roelfsema, C, & Phinn, SR (2009_) Efficient radiative transfer model inversion for remote
 504 sensing applications. *Remote Sensing of Environment*, 113, 2527 – 2532.
- 505 Jenness J. (2006). Radiating Lines and Points (rad_lines.avx) Extension for ArcView 3.x, v. 1.1.
 506 Jenness Enterprises.
- 507 Johannes R.E., Coles S.L., Kuenzel N.T. (1970). The role of zooplankton in the nutrition of some
 508 scleractinian corals. *Limnological Oceanography* 15, 579-586
- 509 Karpouzli E., Malthus, T.J.M. & Place C.J. (2004). Hyperspectral discrimination of coral reef benthic
 510 communities in the western Caribbean. *Coral Reefs* 24, 124-134.
- 511 Kleypas J.A., Buddemeier R.A., Archer D., Gattuso J.P., Langdon C., Opdyke B.N. (1999).
 512 Geochemical consequences of increased atmospheric carbon dioxide on coral reefs. *Science* 284, 118–
 513 120.
- 514 Klonowski, W.M., Fearn, CS and Lynch, MJ (2007) Retrieving key benthic cover types and
 515 bathymetry from hyperspectral imagery, *Journal of Applied Remote Sensing*, 1, 11 – 50.
- 516 Kohler, K.E. and Gill, S.M. (2006). Coral Point Count with Excel extensions (CPCe): A Visual Basic
 517 program for the determination of coral and substrate coverage using random point count methodology.
 518 *Computers and Geosciences*, 32, 1259-1269
- 519 Komar P.D. (1976). Beach processes and sedimentation. New Jersey: Prentice-Hall.
- 520 Kruse F.A., Lefkoff A.B., Boardman J.B., Heidebrecht K.B., Shapiro A.T., Barloon P.J., Goetz A.F.H.
 521 (1993). The Spectral Image Processing System (SIPS) - Interactive visualization and analysis of
 522 imaging spectrometer data. *Remote Sensing of Environment*, 44, 145–163.
- 523 Lee, Z. K. Carder, C. D. Mobley, R. Steward, & Patch, J. (1998). Hyperspectral Remote Sensing for
 524 Shallow Waters. 1. A semi-analytical model. *Applied Optics*, 37, 6329-6338.

- 525 Lee, Z. K. Carder, C. D. Mobley, R. Steward, & Patch, J. (1999). Hyperspectral Remote Sensing for
526 Shallow Waters. 2. Deriving Bottom Depths and Water Properties by Optimization. *Applied Optics*,
527 38, 3831-3843.
- 528 LeDrew E.F., Holden H., Wulder M.A., Derksen C., Newman C. (2004). A spatial statistical operator
529 applied to multirate satellite imagery for identification of coral reef stress. *Remote Sensing of*
530 *Environment*, 91, 271-279.
- 531 Massel S.R. (1996). Ocean surface waves: their physics and prediction. , Singapore and London:
532 World Scientific.
- 533 Ord J.K. (1975). Estimation methods for models of spatial interaction. *Journal of American Statistical*
534 *Association*, 70, 120-126.
- 535 Phinn S.R., Neil, D.T., Joyce K.E. (2000). Coral Reefs: A multi-scale approach to monitoring their
536 composition and dynamics. 30th International Symposium on Remote Sensing of Environment,
537 Honolulu Sheraton, Hawai'i, 2672-2674.
- 538 Purkis S.J., Kohler K.E, Riegl B.M., Rohmann S.E. (2007). The statistics of natural shapes in modern
539 coral reef landscapes. *Journal of Geology*, 115, 493–508.
- 540 Rinkevich B., Loya Y. (1979). The reproduction of the Red Sea coral *Stylophora pistillata*. 1. Gonads
541 and planulae. *Marine Ecology Progress Series*, 1, 133-144.
- 542 Rogers C.S. (1990). Responses of coral reefs and reef organisms to sedimentation. *Marine Ecology*
543 *Progress Series*, 62, 185-202.
- 544 Savitzky, A. & Golay, M.J.E. (1964). Smoothing and Differentiation of Data by Simplified Least
545 Squares Procedures. *Analytical Chemistry*, 36, 1627–1639.
- 546 Schott, J.R. (2007) Remote sensing: The image chain approach, Second Edition. Oxford: Oxford
547 University Press.
- 548 Shaked, Y., Genin, A. (2011) Red Sea and Gulf of Aqaba. In: Hopley D (ed) Encyclopedia of Modern
549 Coral Reefs. Springer, Dordrecht, The Netherlands, p 839.
- 550 Sheppard, C. R. C. (1982) Coral Populations on Reef Slopes and Their Major Controls *Marine*
551 *Ecology Progress Series*, 7, 83-115.
- 552 Sheppard C.R.C., Price A., Roberts C. (1992). Marine ecology of the Arabian region: patterns and
553 processes in extreme tropical environments. London: Academic Press.
- 554 Smirnov O., Anselin L. (2001). Fast maximum likelihood estimation of very large spatial
555 autoregressive models: A characteristic polynomial approach. *Computational Statistics and Data*
556 *Analysis* 35, 301–319.
- 557 Sobel J, Dahlgren C. 2004. *Marine reserves: a guide to science, design and use*. Island Press:
558 Washington DC.
- 559 US Navy (1995). U.S. Navy marine climatic atlas of the world. Volume III: Indian Ocean. Published
560 by direction of the Chief of Naval Operations. U.S. Government Printing Office, Washington, DC
- 561 Veron J.E.N., Pichon M. (1976). Scleractinia of Eastern Australia. Part I. Families Thamnasteriidae,
562 Astrocoeniidae, Pocilloporidae. *Australian Institute of Marine Science Monograph Series*, 1, 1-86
- 563 Wettle, M & Brando, V.E. (2006) SAMBUCA – Semi-Analytical model for Bathymetry, Unmixing
564 and Concentration assessment, CSIRO Land and Water Science Report No. 22/06. CSIRO.

565
566

567 **Figure list**

568

569 Figure 1 Landsat TM image of the Al Wajh Bank, Saudi Arabia, Red Sea (25°39'N, 34°45'E) and the
570 location of the study site (upper inset) and the Al Wajh Bank in the Red Sea (lower inset).

571

572 [Figure 2. Schematic overview of the construction process for the live coral cover model at Al Wajh.]

573

574 Figure 3. Phototransects used for validating benthic estimations derived from the spectral unmixing
575 algorithm, one shallow and one deep transect per site. Locations plotted on the RGB image composite
576 of the study area

577

578 Figure 4 (a) Hyperspectral colour composite imagery of the study area; (b) Gray scale unmixed image
579 output depicting the abundance of coral, white areas indicate areas of high coral cover; (c-e) Spatial

580 distribution of the modelled values for the three explanatory variables: (c) Bathymetry, (d) Wave
 581 power, and (e) Suspended sediment concentration.

582

583 **Table 1.** Constraints employed for optimisation of the semi-analytical inversion model, as defined in
 584 Goodman (2008).

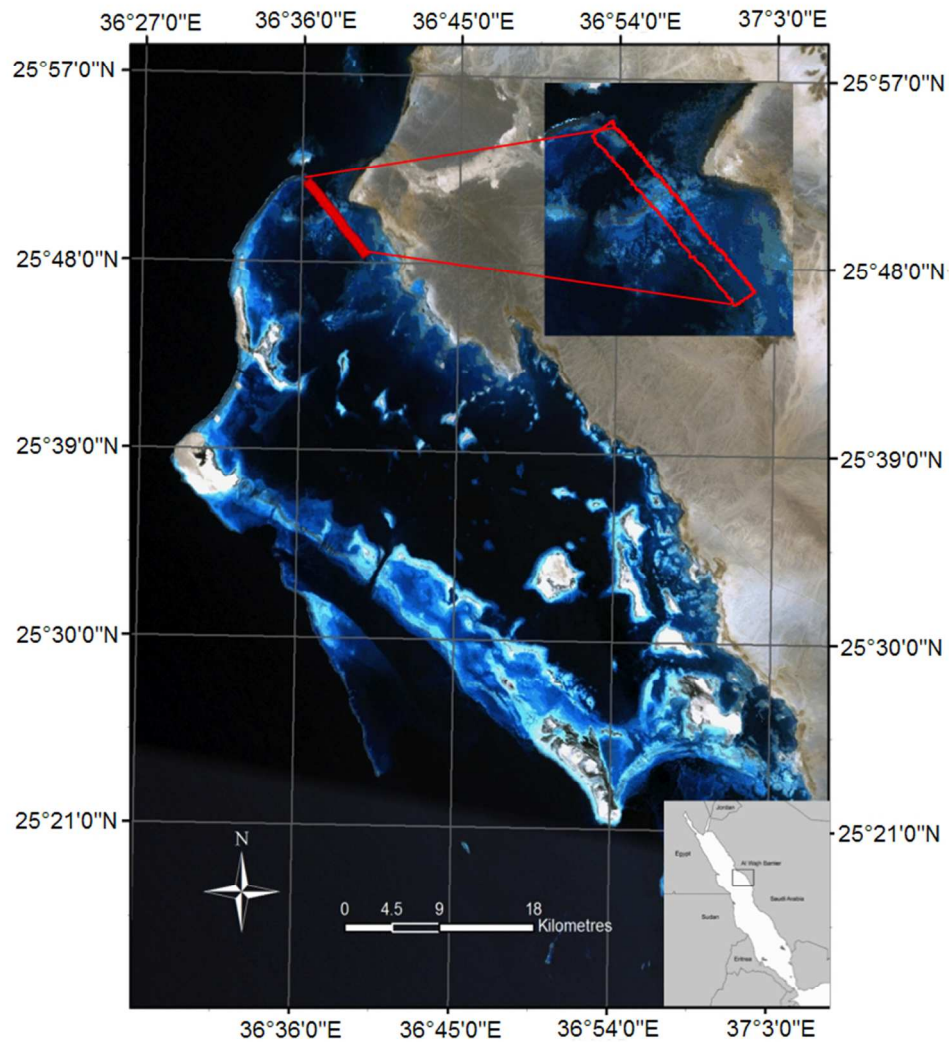
Parameter	Constraint
P (m^{-1}) is the phytoplankton absorption coefficient at 440 nm	$0.005 \leq P \leq 0.5$
G (m^{-1}) = absorption coefficient for gelbstoff and detritus at 440 nm	$0.002 \leq G \leq 3.5$
BP (m) particle-backscattering coefficient	$0.001 \leq BP \leq 0.5$
B is the bottom albedo at 550 nm	$0.01 \leq B \leq 0.6$
H (m) is the bottom depth	$0.2 \leq H \leq 33.0$

585

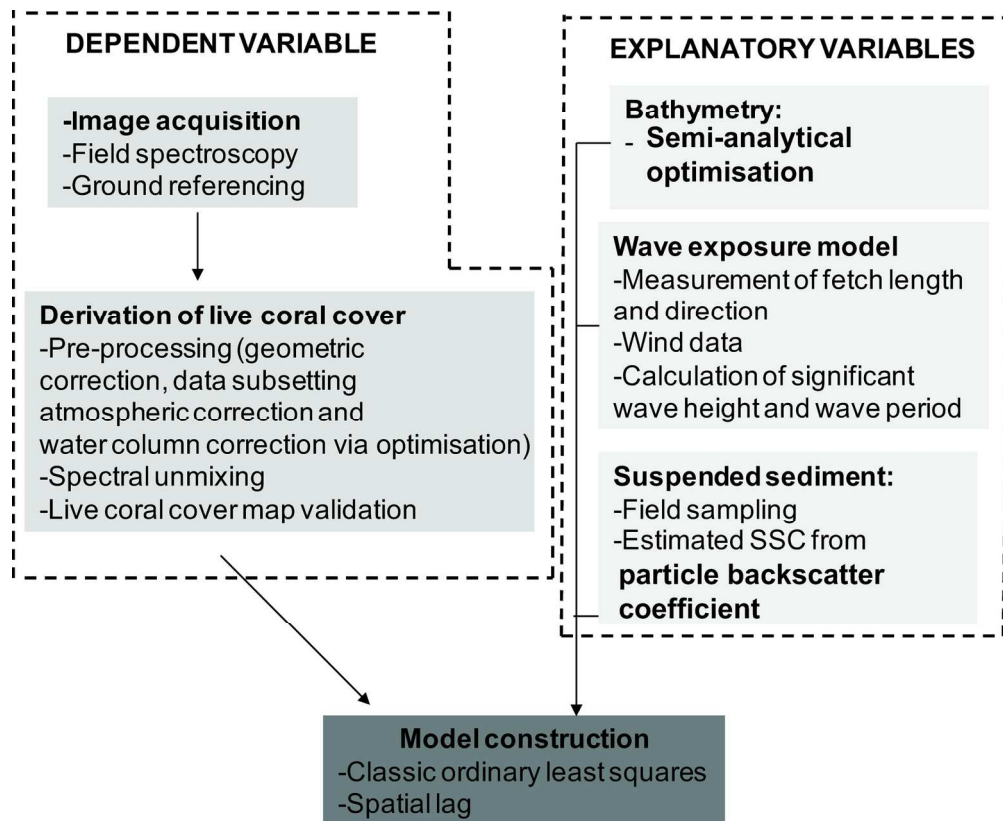
586 **Table 2** Summary of results and diagnostics for the two types of regression.

CLASSIC ORDINARY LEAST SQUARES REGRESSION			
R ² (adjusted value)		0.27 (0.26)	
Moran's I of residuals		0.73	
Variable	β Coefficient	Standard error	t-statistic
Depth	-0.55	0.03	-12.31 (p<0.001)
Suspended sediment	0.96	0.03	27.78 (p<0.001)
Wave power	0.03	0.02	14.74 (p<0.001)
SPATIAL MODEL			
R ²		0.76	
Moran's I of residuals		-0.14	
Variable	β Coefficient	Standard error	t-statistic
Depth	-0.088	0.02	-3.67 (p<0.001)
Suspended sediment	0.168	0.02	8.80 (p<0.001)
Wave power	0.040	0.01	4.15 (p<0.001)

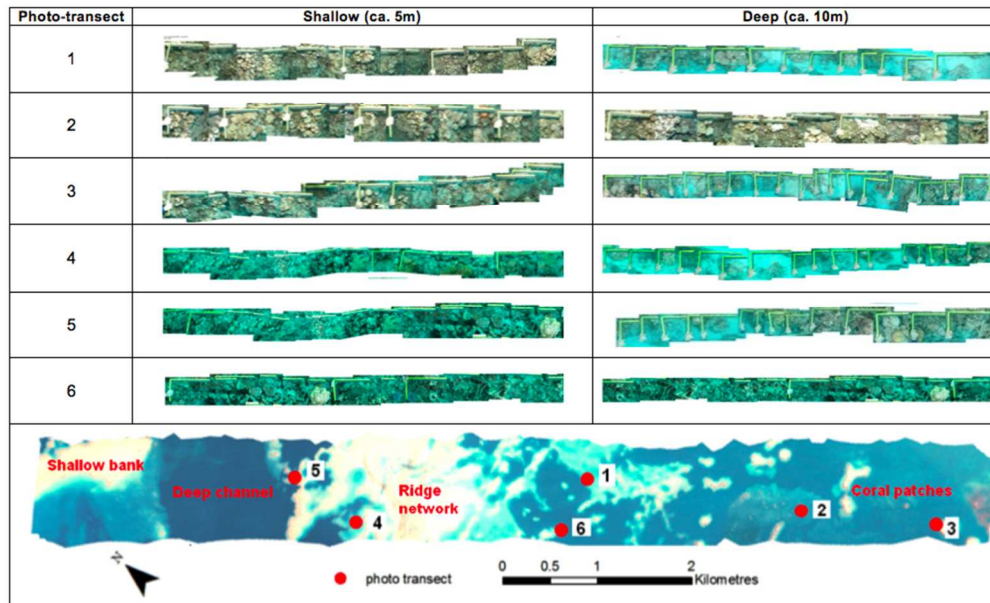
587



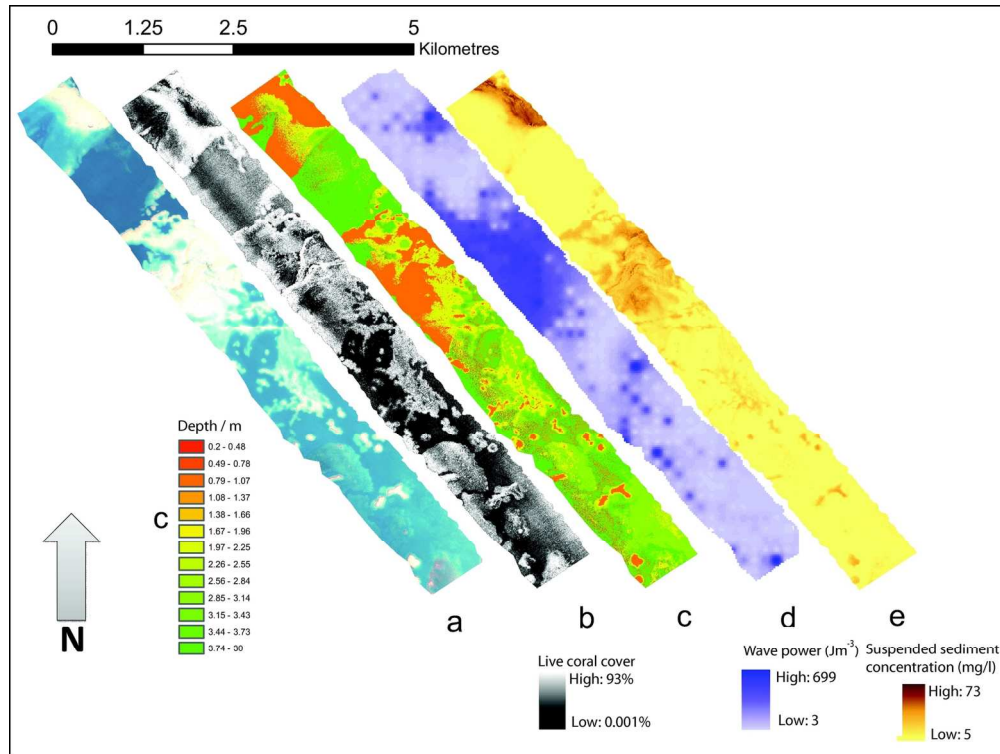
Landsat TM image of the Al Wajh Bank, Saudi Arabia, Red Sea (25°39'N, 34°45'E) and the location of the study site (upper inset) and the Al Wajh Bank in the Red Sea (lower inset). 225x254mm (96 x 96 DPI)



Schematic overview of the construction process for the live coral cover model at Al Wajh.
162x132mm (300 x 300 DPI)



Phototransects used for validating benthic estimations derived from the spectral unmixing algorithm, one shallow and one deep transect per site. Locations plotted on the RGB image composite of the study area 322x195mm (72 x 72 DPI)



a) Hyperspectral colour composite imagery of the study area (RGB wavebands at 767, 519 and 403nm) b) Gray scale unmixed image output depicting the abundance of coral, white areas indicate areas of high coral cover, c-e) Spatial distribution of the modelled values for the three explanatory variables: iii. Bathymetry, iv. Wave power, and v. Suspended sediment concentration.
157x118mm (300 x 300 DPI)